Dynamic Alternations in Cellular and Molecular Components during Blossom-End Rot Development in Tomatoes Expressing sCAX1, a Constitutively Active Ca^{2+}/H^+ Antiporter from Arabidopsis[1][W][OA]

Sergio Tonetto de Freitas, Malkeet Padda, Qingyu Wu, Sunghun Park, and Elizabeth J. Mitcham*

Department of Plant Sciences, University of California, Davis, California 95616 (S.T.d.F., M.P., E.J.M.); and Department of Horticulture, Forestry, and Recreation Resources, Kansas State University, Manhattan, Kansas 66506 (Q.W., S.P.)

Although calcium (Ca) concentration in cellular compartments has been suggested to be tightly regulated, Ca deficiency disorders such as blossom-end rot (BER) in tomato (*Solanum lycopersicum*) fruit may be induced by abnormal regulation of Ca partitioning and distribution in the cell. The objectives of this work were to analyze the effects of high expression of the constitutively functional Arabidopsis (*Arabidopsis thaliana*) Ca^{2+}/H^+ exchanger (sCAX1) tonoplast protein in tomato fruit on cellular Ca partitioning and distribution, membrane integrity, and the transcriptional profile of genes potentially involved in BER development. Wild-type and *sCAX1*-expressing tomato plants were grown in a greenhouse. Wild-type plants did not develop BER, whereas *sCAX1*-expressing plants reached 100% BER incidence at 15 d after pollination. The *sCAX1*-expressing fruit pericarp had higher total tissue and water-soluble Ca concentrations, lower apoplastic and cytosolic Ca concentrations, higher membrane leakage, and Ca accumulation in the vacuole of *sCAX1*-expressing cells. Microarray analysis of healthy *sCAX1*-expressing fruit tissue indicated down-regulation of genes potentially involved in BER development, such as genes involved in membrane structure and repair and cytoskeleton metabolism, as well as up-regulation of genes that may have limited BER damage expansion, such as genes coding for heat shock proteins, glutathione *S*-transferases, and peroxidases. The results indicate that the high expression of the *sCAX1* gene reduces cytosolic and apoplastic Ca concentrations, affecting plasma membrane structure and leading to BER symptom development in the fruit tissue.

Blossom-end rot (BER) is a physiological disorder in tomato (*Solanum lycopersicum*) fruit that starts as water-soaked tissue at the blossom-end region and eventually becomes dark brown and may spread to the whole fruit (Ho and White, 2005). At the tissue level, the first visual symptom of BER is cell plasmolysis, which is always associated with leaky membranes (Simon, 1978; Ho and White, 2005). Although high susceptibility to BER has been associated with lower calcium (Ca) concentration in fruit tissue, total tissue Ca concentration is not a precise predictor of BER development, and frequently, fruit showing BER symptoms have equal or even more Ca than healthy fruit (Nonami et al., 1995; Ho and White, 2005). The high correlation with no predictive accuracy between total tissue Ca and BER incidence is possibly the result of abnormal cellular Ca partitioning and distribution, leading to a localized Ca deficiency within the cell. Understanding the mechanisms involved in BER development is the key to effectively control this disorder, which can reach values higher than 50% incidence, decreasing crop yield, quality, and the return on the effort and investments spent during production (Abdal and Suleiman, 2005).

At the cellular level, the apoplastic Ca concentration must be greater than 0.1 mM Ca to maintain the integrity and selectivity of the plasma membrane, cytosolic Ca concentration must be maintained in the range of 0.1 to 0.2 μM to avoid toxicity, and Ca storage organelles (vacuole, endoplasmic reticulum) must contain 1 to 10 mM Ca, which is required for signaling responses and charge balance (Hanson, 1960; Plieth, 2001; White and Broadley, 2003). Proper cellular Ca partitioning and distribution depends on the activity of a complicated machinery composed of Ca^{2+} channels, H^+/Ca^{2+} exchangers, Ca^{2+}-ATPases, and Ca^{2+} sensors (Cessna and Low, 2001; White and Broadley, 2003). Previous reports suggest that aberrant regulation of cellular Ca partitioning and distribution may lead to Ca deficiency symptom development (Hirschi, 1999; Ho and White, 2005). In these studies, high expression of a constitutively functional Arabidopsis

[1] This work was supported by the Coordenação de Aperfeiçoamento de Pessoal de Nível Superior-Brazil/Fulbright (scholarship to S.T.d.F.) and by the California League of Food Processors.

* Corresponding author; e-mail ejmitcham@ucdavis.edu.

The author responsible for distribution of materials integral to the findings presented in this article in accordance with the policy described in the Instructions for Authors (www. plantphysiol.org) is: Elizabeth J. Mitcham (ejmitcham@ucdavis.edu).

[W] The online version of this article contains Web-only data.

[OA] Open Access articles can be viewed online without a subscription.

www.plantphysiol.org/cgi/doi/10.1104/pp.111.175208

(*Arabidopsis thaliana*) Ca^{2+}/H^{+} exchanger (sCAX1) tonoplast protein in tomato plants not only increased the total amount of Ca in the fruit but also increased by 90% the incidence of the Ca deficiency disorder BER (Park et al., 2005a). The *sCAX1*-expressing tomato phenotypes, in conjunction with the biochemical properties of sCAX1 in yeast (Hirschi et al., 1996; Hirschi, 1999), suggest that expression of this transporter potentially altered Ca partitioning and distribution by increasing the vacuolar Ca level and decreasing the cytosolic and apoplastic Ca levels in the cells. Similar results were also obtained in tobacco (*Nicotiana tabacum*; Hirschi, 1999), carrot (*Daucus carota*; Park et al., 2004), and potato (*Solanum tuberosum*; Park et al., 2005b) by overexpressing vacuolar H^{+}/Ca^{2+} *exchangers*. In these studies, the susceptibility to Ca deficiency development was always positively correlated with the expression level of the H^{+}/Ca^{2+} *exchanger* transgene.

The high flow of Ca into the vacuole of *sCAX1*-expressing cells can potentially deplete the apoplastic pool of Ca, leading to a localized cellular Ca deficiency and death. The apoplastic pool of Ca is required for proper plasma membrane integrity and function by binding to phospholipids and proteins at the membrane surface (Hanson, 1960; Clarkson and Hanson, 1980; Hirschi, 2004). Ca has also been shown to increase membrane phospholipid and monogalactosyldiacylglycerol concentrations and to preserve membrane integrity not only by delaying senescence-related membrane lipid changes but also by increasing membrane-restructuring processes (Picchioni et al., 1996, 1998). Since BER symptoms start with leaky membranes and cell plasmolysis (Ho and White, 2005), an abnormal depletion of the apoplastic pool of Ca in fruit tissue could explain the high incidence of BER observed in *sCAX1*-expressing fruit.

The inability of cells to respond properly to any stimuli dependent on cytosolic Ca oscillations may also be the cause of cell death and BER development in *sCAX1*-expressing tomato fruit. In response to specific biotic and abiotic stimuli, Ca^{2+} channels present in the plasma membrane, tonoplast, and/or endoplasmic reticulum open, allowing Ca to flow into the cytosol (White, 2000). The pattern of Ca influx through channels generates perturbations in the cytosolic Ca concentration that initiate specific cellular responses (White, 2000; Sanders et al., 2002). Particular cytosolic proteins that change conformation or catalytic activity upon binding Ca, such as calmodulin, calcineurin B-like proteins, and Ca-dependent protein kinases, allow the cellular perception and transduction of the specific cytosolic Ca signal (White and Broadley, 2003). The submicromolar concentration of Ca in the cytosol is then reestablished by the activity of high-capacity H^{+}/Ca^{2+} exchangers and high-affinity Ca^{2+}-ATPases. These enzymes are also believed to define the specificity of cell responses by controlling the level of cytosolic Ca oscillation (White and Broadley, 2003). In this context, the high incidence of BER in *sCAX1*-expressing tomato fruit may be the result of a constitutively high flow of Ca into the vacuole, which may affect cytosolic Ca oscillations, and consequently proper cellular responses to biotic and abiotic stimuli, eventually leading to cell death. A transcriptional profile analysis could reveal the possible metabolic processes affected in *sCAX1*-expressing fruit tissue and could also indicate candidate genes involved in BER development.

The mechanism by which the *sCAX1*-expressing tomato fruit triggers BER development may be similar to the mechanism involved in BER development in more susceptible cultivars, which may also have abnormal regulation of Ca partitioning and distribution. Considering that about 40% of the Ca in fruit tissue is located in the vacuole, this organelle is an important regulator of Ca partitioning and distribution in the cell (Rossignol et al., 1977; Harker and Venis, 1991). Imbalanced Ca movement into the vacuole could also explain the fact that fruit with BER frequently have similar or even higher concentrations of total fruit Ca than healthy fruit. The *sCAX1*-expressing tomato plant can be used as a tool to explore and understand the mechanisms involved in BER development in tomato fruit.

Our objectives were to test the hypothesis that high expression of the *sCAX1* gene lowers the apoplastic pool of Ca, which increases membrane leakiness and cell plasmolysis, and triggers BER development. In addition, we expect that high expression of the *sCAX1* gene will lead to altered cytosolic Ca-dependent cellular responses, triggering changes in the expression of genes involved in BER development.

RESULTS

BER Incidence, Membrane Leakage, and Ca Concentrations in Fruit Pericarp Tissue

The *sCAX1*-expressing plants reached 100% BER incidence at 15 d after pollination (DAP), whereas wild-type plants did not develop this disorder during fruit growth and development under our greenhouse conditions (Figs. 1 and 2A). Some *sCAX1*-expressing fruit developed BER symptoms on the entire surface (data not shown). Membrane leakage was higher in *sCAX1*-expressing fruit pericarp tissue compared with the wild type at both 15 and 45 DAP (Fig. 2B). The *sCAX1*-expressing fruit pericarp had lower water-soluble apoplastic Ca concentration but higher total water-soluble and tissue Ca concentrations at both 15 and 45 DAP (Fig. 3). Our confocal microscopy studies showed that *sCAX1*-expressing cells from pericarp without visible BER symptoms had significantly lower steady-state concentrations of cytosolic Ca than wild-type fruit pericarp cells (Fig. 4).

Tissue Structure and Ca Accumulation inside the Vacuole of *sCAX1*-Expressing Cells

Electron microscopy images taken at 15 DAP showed that wild-type and *sCAX1*-expressing fruit pericarp tissue without water-soaked symptoms of

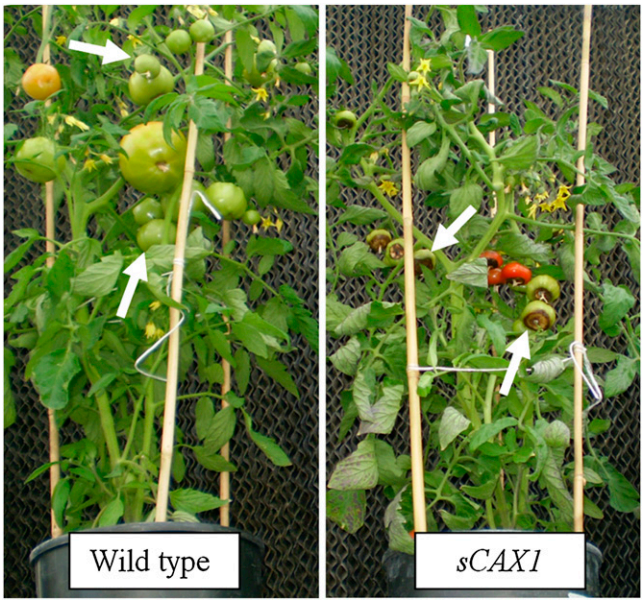

Figure 1. Wild-type and *sCAX1*-expressing cv FM9 phenotypes at 45 DAP. Wild-type plants had no BER incidence, and *sCAX1*-expressing plants showed 100% BER incidence since 15 DAP. White arrows point to 100% healthy fruit in wild-type plants and 100% fruit with BER visual symptoms in *sCAX1*-expressing plants.

BER had turgid cells, whereas *sCAX1*-expressing fruit pericarp with water-soaked symptoms had plasmolyzed epidermal and subepidermal cells (Fig. 5). The epidermal cells of *sCAX1*-expressing fruit had a thicker cuticular layer than the wild-type fruit (Fig. 5, A and B), and the *sCAX1*-expressing fruit with BER symptoms also showed thicker cell walls than the wild-type and the *sCAX1*-expressing fruit pericarp without visible symptoms of BER (Fig. 5C). Electron micrographs with potassium antimonate of *sCAX1*-expressing pericarp cells without visible water-soaking symptoms taken at 15 DAP show the beginning of plasmolysis and aberrant Ca accumulation inside the vacuole of *sCAX1*-expressing pericarp cells, which was not observed in the wild-type pericarp cells (Figs. 6 and 7).

Transcriptional Analysis

Transcriptional profile analysis of healthy *sCAX1*-expressing fruit pericarp, compared with wild-type fruit pericarp at 15 DAP, shows up-regulation of 277 genes, with 2% encoding Ca-binding proteins, 5% proteins involved in signaling pathways, 7% transcription factors, 2% membrane transport, 6% biotic and abiotic stress, 16% oxidation and reduction reactions, 5% protein metabolism and catabolism, 8% carbohydrate metabolism, 3% lipid metabolism, 8% cell wall metabolism, and 1% hormone metabolism (Fig. 8A; Supplemental Table S1). Genes down-regulated in *sCAX1*-expressing fruit pericarp are represented by 3% encoding Ca-binding proteins, 4% proteins involved in signaling pathways, 7% transcription factors, 3% membrane transport, 3% biotic and abiotic stress, 6% oxidation and reduction reactions, 7% protein metabolism and catabolism, 9% carbohydrate metabolism, 4% lipid metabolism, 12% cell wall metabolism, and 4% hormone metabolism (Fig. 8B; Supplemental Table S2). The expression of genes involved in nitrogen metabolism (3%) and photosynthesis (1%) was only up-regulated (Fig. 8A). Transcriptional analysis of healthy *sCAX1*-expressing fruit tissue indicated possible changes in gene expression that may have triggered BER development, such as down-regulation of genes involved in membrane structure and repair (synaptotagmin and dynamin) and cytoskeleton metabolism (GTP-binding protein and actin-binding protein), as well as changes in gene expression that may have limited BER damage expansion in the fruit, such as up-regulation of heat shock proteins, glutathione *S*-transferases, and peroxidases and down-regulation of proteases (Fig. 8; Supplemental Tables S1 and S2).

The metabolomic profile analysis of *sCAX1*-expressing healthy fruit pericarp based on the microarray data suggests an increase in ubiquitin and autophagy degradation pathways (Supplemental Fig. S1), inhibition in the biosynthesis of cell wall precursors (Supple-

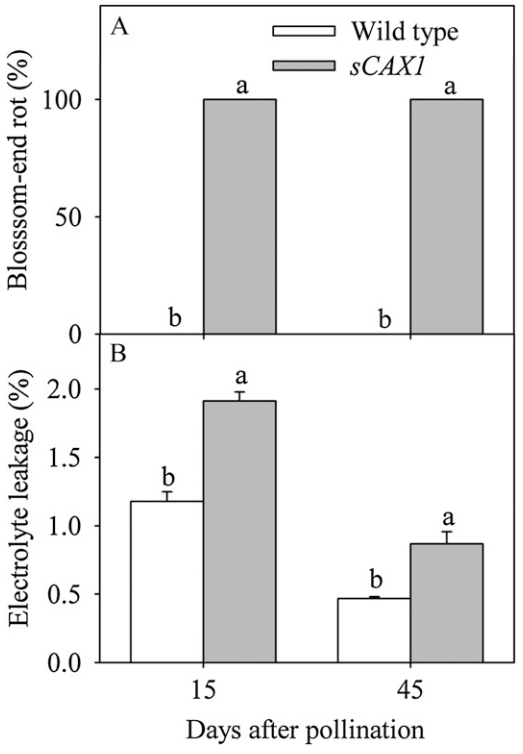

Figure 2. A, BER incidence determined as the percentage of fruit with visual BER symptoms in each replication. B, Electrolyte leakage of pericarp tissue calculated based on the change in conductivity per hour as a percentage of the total conductivity. Wild-type (white bars) and *sCAX1*-expressing (gray bars) tomatoes were assayed. Data were analyzed at 15 and 45 DAP. Mean values with different letters at each time are significantly different according to Duncan's test ($P = 0.05$). For both the wild type and *sCAX1*, $n = 6$. Data shown are means ± SE.

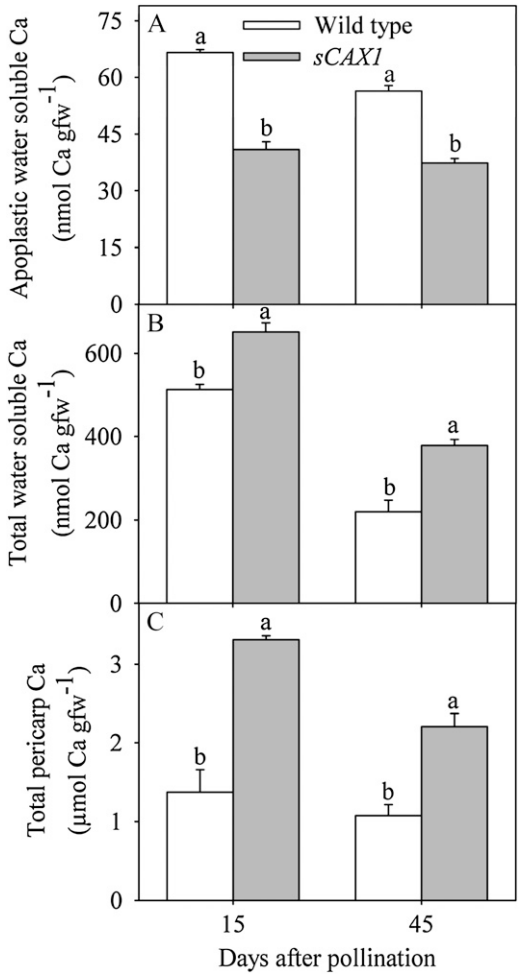

Figure 3. A, Apoplastic water-soluble Ca extracted by vacuum infiltrating an isotonic mannitol solution (0.68 MPa) through pericarp discs. B, Total water-soluble Ca extracted after freezing and thawing pericarp samples. C, Total pericarp tissue Ca concentration. Wild-type (white bars) and *sCAX1*-expressing (gray bars) tomatoes were assayed. Data were analyzed at 15 and 45 DAP. Mean values with different letters at each time are significantly different according to Duncan's test ($P = 0.05$). For both the wild type and *sCAX1*, $n = 6$. Data shown are means ± SE. gfw, Grams fresh weight.

mental Fig. S2), and an increase in phenylpropanoids and lignin biosynthesis (Supplemental Fig. S3).

Expression of Genes Involved in Ca Movement into Cellular Organelles

The expression of the Arabidopsis *sCAX1* gene was not detected in wild-type tomato fruit (Table I). The highest expression of the *sCAX1* gene in *sCAX1*-expressing fruit was observed at 15 DAP, which decreased at 45 DAP (Table I). Since we were also interested in the effects of sCAX1 activity on the expression of other genes involved in Ca movement into cellular organelles, we specifically analyzed the expression of these genes by real-time (RT)-PCR. Expression analysis showed that two putative vacuolar Ca^{2+}/H^+ *exchangers*, *CAX3* and *CAX6*, and one putative Ca^{2+}/Na^+ *exchanger*, *CAX7*, had lower expression in *sCAX1*-expressing fruit pericarp without visible BER symptoms compared with wild-type fruit pericarp (Table II). One Ca^{2+}/H^+ *exchanger*, *CAX4*, was more highly expressed in *sCAX1*-expressing fruit pericarp than in the wild type (Table II). Among eight putative Ca-ATPases, seven had lower expression in *sCAX1*-expressing fruit pericarp tissue and one (Ca-ATPase5) had similar expression in both wild-type and *sCAX1*-expressing fruit pericarp tissue (Table II). The *sCAX1*-expressing fruit pericarp had lower expression of a putative H^+ *pyrophosphatase* (*VPPase*) and a *Vacuolar-ATPase* (*V-ATPase*) during fruit growth and development (Table II).

DISCUSSION

Cellular Ca Partitioning and Distribution and BER Development in *sCAX1*-Expressing Fruit

BER is believed to be caused by Ca deficiency in tomato fruit tissue (Ho and White, 2005). This assumption is based on the facts that (1) growing tomato plants under hydroponic conditions with low Ca results in BER development, (2) fruit with BER symptoms usually have lower Ca concentrations, and (3) spraying fruit and plants with Ca solutions reduces the probability of BER development (Evans and Troxler, 1953; Geraldson, 1957; Millikan et al., 1971). Although there is strong evidence supporting the role of Ca in BER development, often fruit that develop BER contain higher levels of Ca than fruit without BER grown under the same agronomic conditions (Nonami et al., 1995; Saure, 2001). Our results show that, in the pericarp tissue, *sCAX1*-expressing fruit had higher total and water-soluble Ca concentrations than the wild-type fruit. However, the *sCAX1*-expressing fruit also showed 100% BER incidence, lower cytosolic and apoplastic Ca concentrations, and an abnormal Ca accumulation inside the vacuole. These results suggest that BER may not be triggered only by low total fruit Ca content but also by an abnormal Ca partitioning and distribution at the cellular level. These ideas appear to contradict previous studies showing that cellular Ca partitioning and distribution is a tightly regulated process (Cessna and Low, 2001; Zhou et al., 2009). However, BER is a physiological disorder, which, by definition, means that it is caused by an abnormal cell metabolism that leads to tissue damage. In this case, the altered metabolism may result from abnormal regulation of cellular Ca partitioning and distribution, resulting in a cellularly localized Ca deficiency and eventually BER development. Previous studies have consistently shown that increasing the expression of vacuolar *CAX* genes not only increased total tissue Ca content but also the incidence and severity of Ca deficiency symptoms in tobacco (Hirschi, 1999), carrot (Park et al., 2004), potato (Park et al., 2005b), and tomato (Park et al., 2005a).

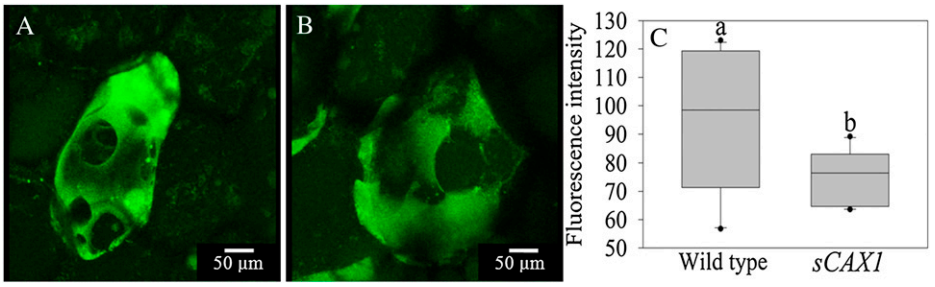

Figure 4. A and B, Projection of three-dimensional images of Fluo4-AM fluorescence in the cytosol of wild-type (A) and *sCAX1*-expressing (B) fruit pericarp cells at 40 DAP. C, Fluorescence intensities of wild-type and *sCAX1*-expressing fruit pericarp cells. Higher fluorescence intensity means higher cytosolic Ca concentration. Mean values are significantly different according to Duncan's test ($P = 0.05$). For both the wild type and *sCAX1*, $n = 5$. Data presented show the fluorescence intensity distribution of 15 cells from five replications (three cells per replication) of wild-type or *sCAX1*-expressing fruit. Top of box, Intensity with 75th percentile; middle line of box, median intensity; bottom of box, intensity with 25th percentile. Points indicate outliers.

Membrane Damage during BER Development

The requirement of Ca for proper membrane structure and function has been well documented in the literature, and fruit tissue with lower Ca content and Ca deficiency symptoms have been reported to have higher membrane leakage (Hanson, 1960, 1984; Simon, 1978; Clarkson and Hanson, 1980; Enoch and Glinka, 1983; Picchioni et al., 1996, 1998; Saure, 2001; Kaya et al., 2002; Hirschi, 2004; Tuna et al., 2007). Accordingly, our results suggest that BER development in *sCAX1*-expressing fruit may begin with increasing membrane permeability followed by plasmolysis of epidermal and subepidermal cells, which result in water-soaked BER symptoms on the fruit surface and finally cell death. This idea is supported by the high correlation observed between cell membrane leakage and BER incidence ($r = 0.95$). Although total Ca concentration was higher in *sCAX1*-expressing fruit than in wild-type fruit, the lower apoplastic Ca concentration observed in *sCAX1*-expressing fruit pericarp was highly correlated with higher membrane leakage ($r = -0.95$) and BER incidence ($r = -0.99$), suggesting that BER could be the result of altered regulation of Ca partitioning and distribution in the *sCAX1*-expressing cells. In this case, the constitutive high expression and activity of the vacuolar sCAX1 protein would favor a "vacuolation" of tissue Ca, reducing the apoplastic pool of this nutrient and increasing membrane leakiness, cell plasmolysis, and BER incidence. This speculation is further supported by the observed high accumulation of Ca inside the vacuole of *sCAX1*-expressing cells. It has been reported before that apoplastic Ca sensors can induce Ca release from cellular organelles into the apoplast when the cell is exposed to lower apoplastic Ca conditions, which reestablish the proper cellular Ca partitioning and distribution (Cessna and Low, 2001). However, *sCAX1*-expressing cells may not be able to regulate Ca partitioning and distribution because of the constitutive high expression and activity of the vacuolar sCAX1 protein.

The transcriptional analysis revealed that the expression of genes involved in membrane structure and repair was down-regulated in *sCAX1*-expressing fruit pericarp. One of these was a putative synaptotagmin, which is a Ca sensor that regulates vesicle exocytosis and endocytosis and mediates the delivery of intracellular membranes to wound sites (Schapire et al., 2008; Lewis and Lazarowitz, 2010). Down-regulation of synaptotagmin has been shown to reduce the viability of cells as a consequence of a decrease in the integrity of the plasma membrane (Schapire et al., 2008). Another observed down-regulated gene was a putative dynamin, which is a GTPase responsible for endocytosis and involved in the scission of newly formed vesicles from the membrane of one cellular compartment and their targeting to, and fusion with, another compartment, both at the cell surface and at the Golgi apparatus (Henley et al., 1999). Down-regulation of dynamins has been shown to cause problems in polar cell expansion, cell plate biogenesis,

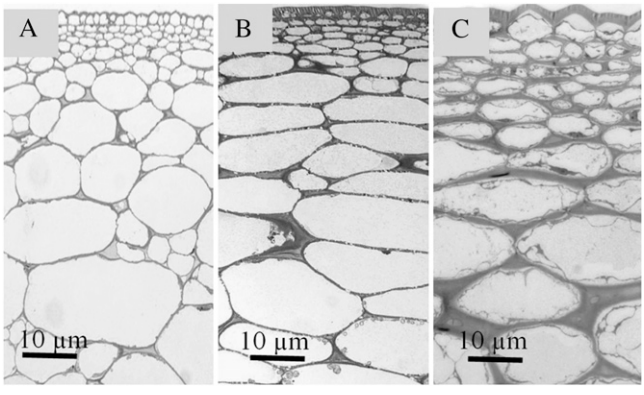

Figure 5. Electron microscopy images of epidermal and subepidermal cells of wild-type fruit pericarp (A), *sCAX1*-expressing healthy fruit pericarp (B), and *sCAX1*-expressing water-soaked fruit pericarp (C) at 15 DAP. Images shown represent averages of 15 images taken on five single fruit replications of each phenotype (three images per fruit).

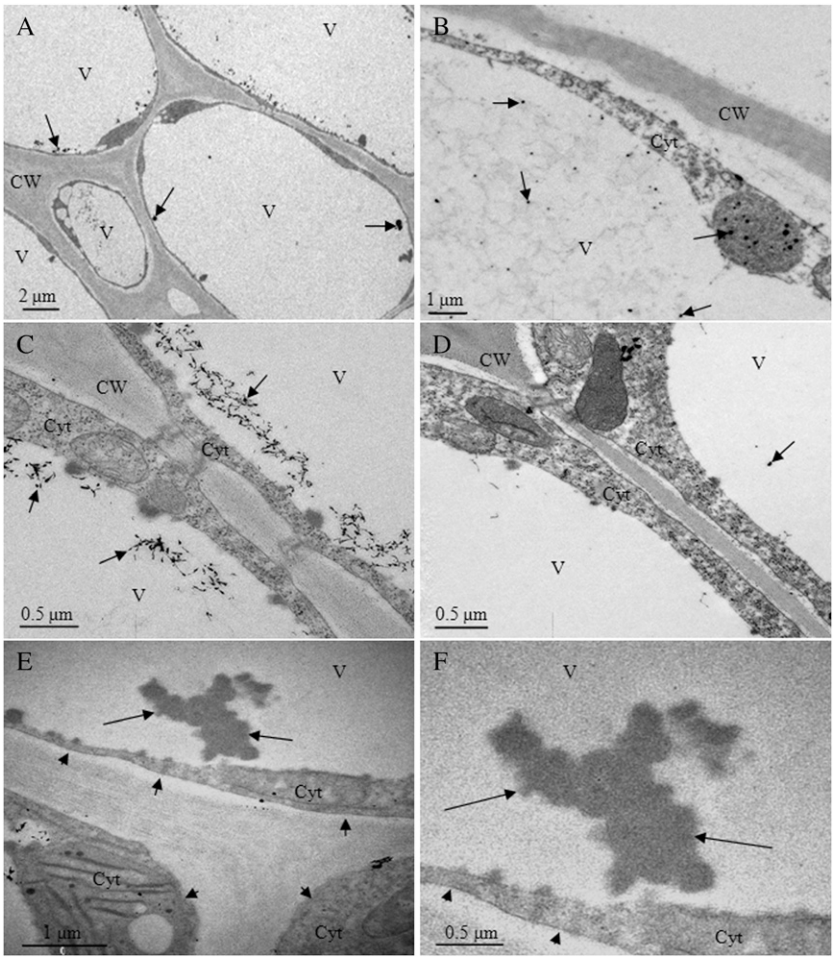

Figure 6. Electron microscopy images of wild-type fruit pericarp cells at 15 DAP. A to D, Arrows point to black spots resulting from the reaction between potassium antimonate and Ca, showing cells with Ca accumulation inside the vacuole. E and F, Arrowheads indicate stretched membranes pressed against the cell wall, and arrows point to similar structures found inside the vacuole of *sCAX1*-expressing cells without potassium antimonate-Ca black spots. The view in E is amplified (2×) in F. CW, Cell wall; Cyt, cytosol; V, vacuole. Images shown represent averages of 15 images taken on five single fruit replications of each genotype (three images per fruit).

and plasma membrane recycling (Kang et al., 2003). Therefore, it is possible that the high expression of the *sCAX1* gene, which reduced the steady-state cytosolic Ca and apoplastic Ca concentrations in tomato fruit, may have also affected cellular processes responsible for proper membrane structure and integrity. In this case, the reduction in the expression of synaptotagmin and dynamin genes could also result in the leaky membranes and cell plasmolysis observed in *sCAX1*-expressing fruit tissue during BER development.

Altered Ca-Dependent Cell Responses in *sCAX1*-Expressing Fruit

Cytosolic Ca oscillations are part of complex cellular responses to abiotic and biotic stimuli, and the specificity of the response is determined by the pattern of cytosolic Ca perturbation (White, 2000; Sanders et al., 2002). In our work, the high expression of constitutively functional sCAX1 tonoplast protein reduced the steady-state cytosolic Ca concentration and possibly resulted in fruit cells unable to respond properly to different stimuli dependent on cytosolic Ca oscillations. The inability to respond properly to different stimuli may be one possible explanation for the observed cell death and BER development mainly at the blossom end of the fruit, which contains the highest rates of cell division and consequently activity of the *cdc2a* promoter (*cdc2a*::*sCAX1*). The results show a reduction in the expression of tomato Ca^{2+}/H^{+} and Ca^{2+}/Na^{+} transporters, *Ca-ATPases*, *V-ATPase*, and *VPPase* genes in *sCAX1*-expressing fruit. The high activity of the sCAX1 protein may have triggered an inhibition in the expression of tomato genes also involved in Ca movement into storage organelles. This mechanism could attempt to reduce the intensity of Ca transport into organelles and allow proper Ca oscillations in the cytosol and cellular responses to different stimuli.

Furthermore, the *sCAX1*-expressing fruit tissue showed a reduction in the expression of cytoskeleton-associated proteins, such as a GTP-binding protein involved in microtubule-dependent transport pathways through the Golgi and from endosomes to the Golgi, and an actin-binding protein involved in actin cytoskeleton organization. Cytosolic Ca oscillations have been reported to trigger microtubule depolymerization and cytoskeletal orientation and reorganization, which in some cases are required for changes in plasma membrane composition (Orvar et al., 2000; Hepler, 2005; Tuteja and Mahajan, 2007). Therefore, the

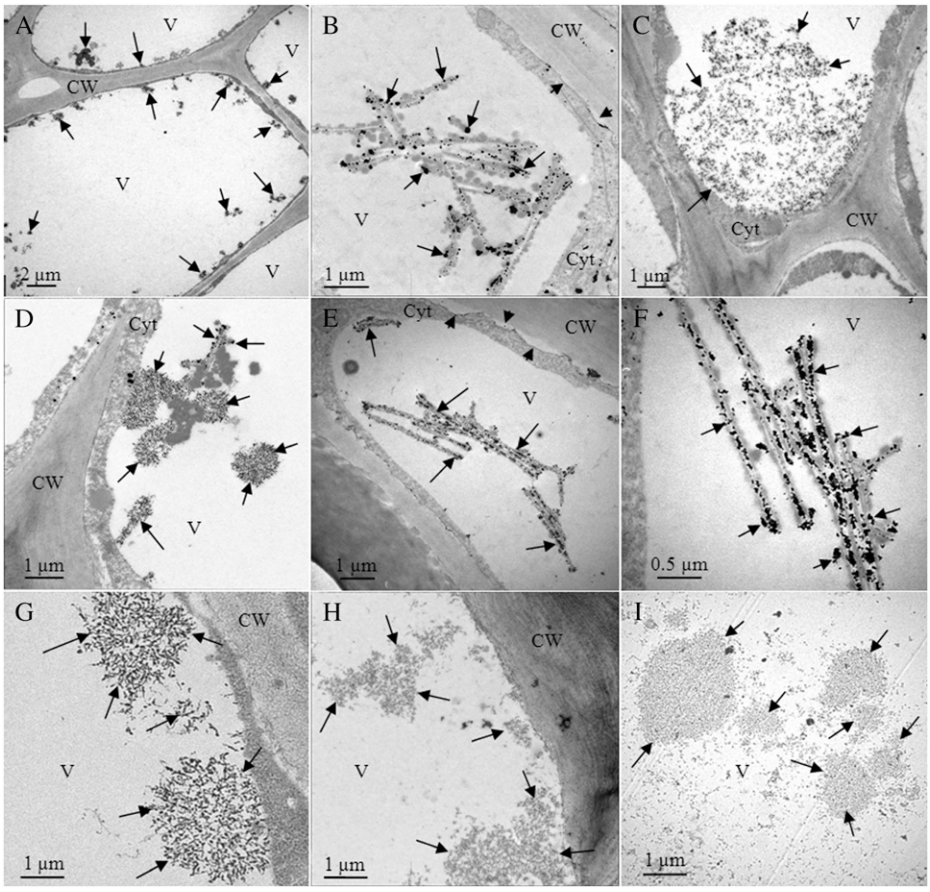

Figure 7. Electron microscopy images of *sCAX1*-expressing fruit pericarp cells without visible BER symptoms at 15 DAP. A to G, Arrows point to black spots resulting from the reaction between potassium antimonate and Ca, showing cells with Ca accumulation inside the vacuole, and arrowheads indicate waved membrane detachment from the cell wall, suggesting the beginning of cell plasmolysis. The view in E is amplified (2.5×) in F. H and I, *sCAX1*-expressing cells after EGTA treatment. Arrows show regions where Ca was removed by EGTA treatment. CW, Cell wall; Cyt, cytosol; V, vacuole. Images shown represent averages of 15 images taken on five single fruit replications of each genotype (three images per fruit).

down-regulation of genes involved in cytoskeleton metabolism as well as membrane structure and repair (discussed in the previous section) could be a consequence of an inability of Ca sensors to detect proper cytosolic Ca oscillations or sense improper cytosolic Ca oscillations because of the high activity of the sCAX1 protein. This idea is supported by the lower steady-state cytosolic Ca concentration observed in *sCAX1*-expressing fruit cells. Alternatively, the down-regulation of these genes could be triggered by factors other than altered cytosolic Ca oscillations, which could also lead to metabolic defects and cell death. Although there is evidence suggesting that the *sCAX1* gene affected cytosolic Ca signaling responses, further work should measure cytosolic Ca oscillations in response to a known, specific stimulus. Under stimulus, cytosolic Ca oscillations can be monitored with Ca-specific fluorophores, such as Fluo-4:acetoxymethyl ester (Fluo4-AM), and the effect of the sCAX1 protein on cellular responses can be further elucidated (Zhang et al., 2010).

Recycling Pathways

The results suggest that *sCAX1*-expressing cells triggered mechanisms to recycle nutrients and carbohydrates. The results show high expression of genes involved in ubiquitin- and autophagy-dependent degradation pathways, which could be necessary to recycle nonfunctional proteins and other cellular products in *sCAX1*-expressing cells. The high activity of these pathways and possibly the uptake of nitrogen from dying cells into healthy cells could also explain the higher expression of genes involved in nitrogen metabolism observed in healthy *sCAX1*-expressing pericarp. In this case, the accumulation of high levels of nitrogen and nitrogen-containing compounds in healthy *sCAX1*-expressing cells may have triggered the increase in expression of nitrate and ammonium transporters, Glu synthase, Glu dehydrogenase, and aminotransferase. The results also show reduction in the expression of enzymes involved in the biosynthesis of cell wall precursors and increase in the expression of UDP-glycosyltransferases, which suggest that healthy cells were possibly redirecting carbohydrates to other pathways. Accordingly, 41 genes coding for enzymes involved in phenylpropanoid biosynthesis (lignin biosynthesis) were up-regulated in healthy *sCAX1*-expressing cells. The activities of recycling pathways and lignin biosynthesis have also been reported before in response to pathogen infection, mechanical damage, and abiotic stress (Love et al., 2008; Shulaev et al., 2008).

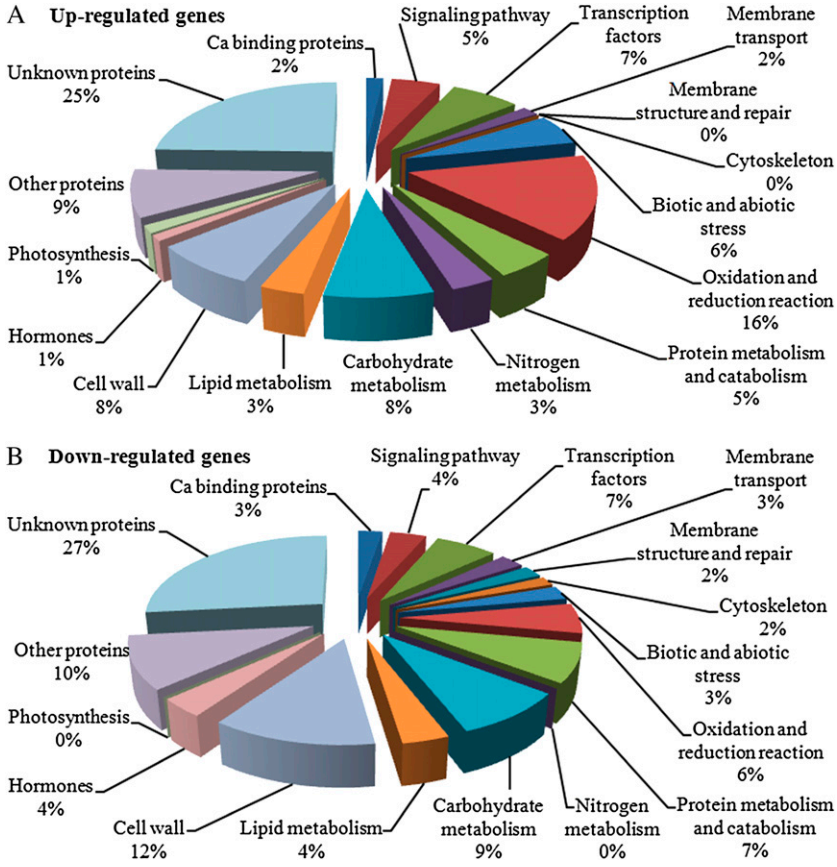

Figure 8. Graphic representation of the percentage of genes belonging to a given functional group for the 277 up-regulated (A) and 229 down-regulated (B) genes in *sCAX1*-expressing fruit pericarp at 15 DAP presented in Supplemental Tables S1 and S2. Level of significance was determined by $P < 0.05$ and paired *t* tests. Only significant expression levels higher than 2-fold are presented. For both the wild type and *sCAX1*, $n = 3$.

Mechanisms Triggered to Reduce BER Symptom Expansion

The transcriptional analysis revealed that healthy *sCAX1*-expressing pericarp tissue close to pericarp tissue showing visual BER symptoms had higher expression of proteins that could suppress cell death and the expansion of BER development in the fruit. Healthy *sCAX1*-expressing fruit pericarp showed higher expression of eight glutathione *S*-transferases, which are enzymes that detoxify endobiotic and xenobiotic compounds by covalent linking of glutathione to hydrophobic substrates (Edwards et al., 2000). Glutathione *S*-transferases are highly expressed under biotic and abiotic stress conditions, and high levels of these enzymes have been shown to reduce the effect of chilling and salt stresses (Roxas et al., 1997). Since stress-inducible glutathione *S*-transferases have been shown to conjugate metabolites arising from oxidative damage, such as fatty acid oxidation (Edwards et al., 2000), high levels of these enzymes in healthy *sCAX1*-expressing pericarp tissue might have limited the expansion of BER symptoms by reducing the accumulation of toxic compounds in healthy cells close to the damaged tissue (Fig. 9).

The expression of six peroxidases was also up-regulated in healthy *sCAX1*-expressing fruit pericarp. Peroxidases have several physiological functions, such as removal of hydrogen peroxide, oxidation of toxic reductants, biosynthesis and degradation of lignin, auxin catabolism, defensive responses to wounding, and defense against pathogen or insect attack (Yoshida et al., 2003). The high levels of peroxidases in healthy *sCAX1*-expressing fruit pericarp close to damaged tissue is likely also part of the defense mechanism to avoid the accumulation of toxic compounds that could eventually cause cell death and the expansion of BER symptoms on the fruit surface (Fig. 9).

The expression of genes encoding proteins involved in protein metabolism and catabolism showed a trend toward maintaining protein stability and inhibiting protein degradation in healthy *sCAX1*-expressing pericarp tissue. This result is supported by the ob-

Table I. *Expression of the sCAX1 gene in tomato fruit*

Data shown are means ± SE. ND, Not detected. For both the wild type and *sCAX1*, $n = 3$.

Tomato	Expression			
	15 DAP	SE	45 DAP	SE
Wild type	ND	±0.00	ND	±0.00
sCAX1	1.00	±0.02	0.58	±0.16

Table II. *Expression of tomato fruit vacuolar CAXs, vacuolar/endoplasmic reticulum Ca-ATPases, VPPase, and V-ATPase*

Different letters in a column indicate statistical differences according to Duncan's test ($P = 0.05$). Data shown are means ± SE. For both the wild type and *sCAX1*, $n = 3$.

Tomato	15 DAP	SE	45 DAP	SE
CAX3				
Wild type	1.00 a	±0.12	1.92 a	±0.08
sCAX1	0.65 b	±0.16	1.35 b	±0.11
CAX4				
Wild type	1.00 b	±0.06	0.76 b	±0.17
sCAX1	1.61 a	±0.18	2.29 a	±0.18
CAX6				
Wild type	1.00 a	±0.05	1.49 a	±0.10
sCAX1	0.94 a	±0.09	1.15 b	±0.03
CAX7				
Wild type	1.00 a	±0.09	0.76 a	±0.03
sCAX1	0.34 b	±0.03	0.45 b	±0.05
Ca-ATPase 1				
Wild type	1.00 a	±0.09	1.66 a	±0.06
sCAX1	0.43 b	±0.04	1.16 b	±0.09
Ca-ATPase 2				
Wild type	1.00 a	±0.05	1.01 a	±0.07
sCAX1	0.67 b	±0.05	0.51 b	±0.01
Ca-ATPase 3				
Wild type	1.00 a	±0.07	1.40 a	±0.15
sCAX1	0.43 b	±0.09	0.49 b	±0.02
Ca-ATPase 4				
Wild type	1.00 a	±0.23	4.09 a	±0.36
sCAX1	0.55 b	±0.14	1.23 b	±0.33
Ca-ATPase 5				
Wild type	1.00 a	±0.21	1.45 a	±0.07
sCAX1	0.77 a	±0.15	1.52 a	±0.18
Ca-ATPase 6				
Wild type	1.00 a	±0.08	1.66 a	±0.21
sCAX1	0.57 b	±0.11	0.72 b	±0.11
Ca-ATPase 7				
Wild type	1.00 a	±0.11	2.36 a	±0.06
sCAX1	0.68 b	±0.13	1.30 b	±0.17
Ca-ATPase 8				
Wild type	1.00 a	±0.15	3.91 a	±0.26
sCAX1	0.67 b	±0.09	1.32 b	±0.12
VPPase				
Wild type	1.00 a	±0.03	0.97 a	±0.04
sCAX1	0.44 b	±0.05	0.51 b	±0.01
V-ATPase				
Wild type	1.00 a	±0.14	2.74 a	±0.11
sCAX1	0.68 b	±0.14	0.86 b	±0.07

served up-regulation in the expression of five heat shock proteins and down-regulation of 10 proteases (proteinases, peptidases) in *sCAX1*-expressing pericarp tissue. Abiotic stresses usually cause protein dysfunction. Maintaining functional conformation of proteins and preventing protein aggregations are particularly important for cell survival under stresses. Heat shock proteins/chaperones are responsible for protein folding, assembly, and translocation in many cellular processes, stabilizing proteins and membranes and assisting in protein refolding under stress conditions. They may play a crucial role in protecting cells against stress by reestablishing normal protein conformation and thus cellular homeostasis (Wang et al., 2004; Fig. 9).

Mechanisms Involved in BER Development

The data presented suggest that high Ca accumulation in storage organelles of *sCAX1*-expressing cells resulted in lower apoplastic Ca concentration and defects in metabolic processes responsible for proper membrane structure and integrity, which led to leaky membranes and BER development (Fig. 9). The high activity of the vacuolar sCAX1 protein may also have affected cytosolic Ca oscillations and Ca-dependent cellular responses to different stimuli, which could also result in cell death and BER development (Fig. 9).

The results suggest that *sCAX1*-expressing cells triggered mechanisms to limit the expansion of BER damage (Fig. 9). Among these mechanisms were the synthesis of glutathione *S*-transferases and peroxidases involved in cell detoxification, synthesis of heat shock proteins to maintain protein stability, and inhibition of protease synthesis to reduce protein degradation. The *sCAX1*-expressing tomato cells also adjusted their metabolism to recycle nutrients and carbohydrates through the ubiquitin- and autophagy-dependent degradation pathways and reincorporate nitrogen by increasing the expression of nitrate and ammonium transporters, Glu synthase, Glu dehydrogenase, and aminotransferase. Possibly, *sCAX1*-expressing cells close to BER damage switched the flow of carbon from cell wall biosynthesis into lignin biosynthesis, which has been reported to be a stress response in plants (Shulaev et al., 2008).

Although the Affymetrix GeneChip interrogates only approximately 9,200 tomato genes, it was a powerful tool to aid our understanding of possible metabolic changes in *sCAX1*-expressing fruit tissue that

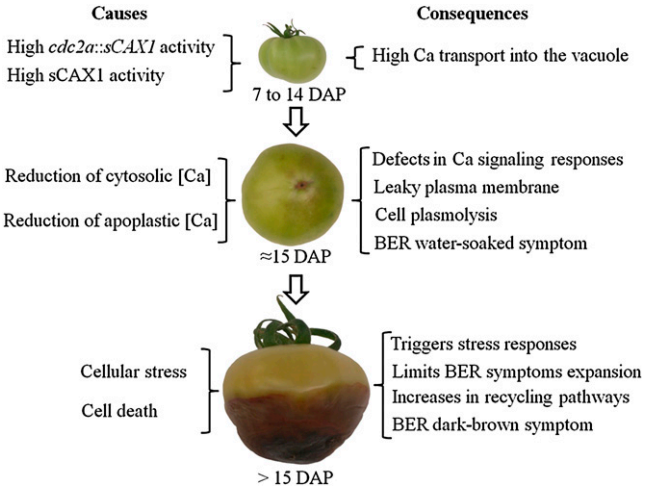

Figure 9. Proposed mechanisms involved in BER development and suppression of BER symptom expansion in *sCAX1*-expressing tomato fruit.

may have led to BER development. Gene-silencing experiments and studies at the protein level should be accomplished to narrow down these results and possibly identify the gene(s) involved in BER development in *sCAX1*-expressing fruit.

MATERIALS AND METHODS

Experimental Procedures

The experiment was accomplished with wild-type and transformed tomato plants (*Solanum lycopersicum* 'FM9'). Transformed plants have an Arabidopsis (*Arabidopsis thaliana*) *sCAX1* transgene without the N-terminal regulatory region, which makes the protein constitutively functional. The *sCAX1* gene is under the control of the cell cycle promoter *cdc2a* (Park et al., 2005a). Since the homozygous plants for the transgene *cdc2a*::*sCAX1* fail to reach flowering because of the high severity of Ca deficiency, only heterozygous plants were used in this study. Both wild-type and *sCAX1*-expressing tomato plants were grown in 9.5-L pots containing organic substrate (0.33% peat, 0.33% sand, 0.33% redwood compost with 2.6 kg dolomite lime m^{-3}) in a greenhouse environment during the spring season at about 20°C day and 18°C night temperatures without supplemental light. The plants were irrigated every day with a fertilizing solution containing nitrogen (102 mg L^{-1}), phosphorus (26 mg L^{-1}), potassium (124 mg L^{-1}), Ca (90 mg L^{-1}), magnesium (24 mg L^{-1}), sulfur (16 mg L^{-1}), iron (1.6 mg L^{-1}), manganese (0.27 mg L^{-1}), copper (0.16 mg L^{-1}), zinc (0.12 mg L^{-1}), boron (0.26 mg L^{-1}), and molybdenum (0.016 mg L^{-1}). At full bloom, fully opened flowers were selected, tagged, and manually pollinated on each plant to monitor the chronological age of the fruit. Fruit samples were harvested and analyzed at 15, 40, and 45 DAP. All parameters were evaluated on six replicated samples, with one plant per replication. The only exceptions were the gene expression, cytochemical, and ultrastructural observations of cellular Ca localization and the cytosolic Ca analysis, which are described below. BER incidence was analyzed by counting the total number of tagged fruit and the number of tagged fruit with visible BER symptoms. Wild-type plants had no BER incidence, and only healthy fruit were analyzed. The *sCAX1*-expressing plants reached 100% BER development at about 15 DAP, and only fruit with early symptoms of BER water soaking were analyzed. In fruit with visible BER symptoms (*sCAX1*-expressing fruit), pericarp samples with skin tissue were taken at the blossom-end region using tissue adjacent to, but not yet affected by, the expanding tissue damage. Healthy fruit (wild-type fruit) were sampled at the exact same position. Fruit samples were evaluated for BER incidence, membrane leakage, total tissue, water-soluble, and apoplastic Ca concentrations, cytochemical and ultrastructural observations of Ca localization in cellular organelles, Affymetrix tomato GeneChip analysis, and expression of putative *CAX* genes, putative *Ca-ATPase* unigenes, a *V-ATPase* gene, and a putative *VPPase* gene.

Membrane Leakage Analysis and Extraction of Total Water-Soluble Ca

Electrolyte leakage was determined in three fruit discs of 1 cm diameter and 0.7 cm thickness (approximately 3 g fresh weight) cut at the blossom end of the fruit with a stainless steel cork borer and sectioned with a double-bladed knife 1 mm under the skin. Each sample of three discs from three fruit represented one replication and was placed into a 50-mL conical tube containing a mannitol solution with similar water potential to the disc tissue (0.68 MPa), and the conductivity was recorded periodically during 6 h. After 6 h, the samples were frozen and thawed twice to determine total conductivity. The values were expressed as a percentage of the total conductivity (Saltveit, 2002). After all measurements, each replication was filtered and the solution collected was used to determine the total water-soluble Ca in the tissue. The tissue water potential was measured by incubating pericarp discs in solutions containing different concentrations of mannitol. The tissue water potential was determined as the solution that maintained a constant tissue weight during incubation.

Apoplastic Ca Extraction and Ca Analysis

Pericarp tissue samples were frozen in liquid N_2 and freeze dried. Samples were subjected to microwave acid digestion and dissolution and analyzed for Ca by inductively coupled plasma atomic emission spectrometry (Meyer and Keliher, 1992). To determine water-soluble apoplastic Ca concentration, 12 fruit discs of 1 cm diameter and 0.3 cm thickness (total of approximately 11 g fresh weight) were cut from the blossom end of the fruit with a stainless steel cork borer and sectioned with a double-bladed knife beginning 1 mm under the skin. Each sample of 12 discs, two discs from each of six fruit, represented one replication. After cutting, each disc was rinsed in deionized water for 10 s and blotted. Blotting the discs after cutting was required to reduce tissue contamination with Ca from the cut surface, as suggested in other studies (Wada et al., 2008). Each disc was then placed in a funnel containing a flat acrylic membrane (1.2 cm diameter) with a pore size of 10 to 16 μm (Kimax; Kimble). The funnel was placed in a Kitasato flask (Pyrex), and vacuum (10–15 mm mercury) was applied. An isotonic mannitol solution (0.68 MPa, 300 μL) was slowly dripped over the entire disc surface and collected in the Kitasato flask. After repeating the procedure for all 12 fruit discs, the mannitol solution accumulated was used for Ca quantification, representing the water-soluble apoplastic Ca content. The procedure was conducted at 4°C. Cell damage was not detected with a light microscope (Olympus SZH10) by analyzing samples before and after the extraction of water-soluble apoplastic Ca extraction. The method described here was chosen after extensive testing of methods described in previous studies (Welbaum and Meinzer, 1990; Pomper and Breen, 1995; Ruan et al., 1995; Olivieri et al., 1998; Almeida and Huber, 1999; Wada et al., 2008).

Cytochemical and Ultrastructural Observations of Cellular Ca Localization

Observations of Ca localization were made with pericarp tissue collected at the blossom-end region of each of five single fruit replications of wild-type or *sCAX1*-expressing genotype. Each single fruit replication was harvested from a different plant at 15 DAP. Pericarp tissue was fixed in 4% glutaraldehyde in 0.1 M potassium phosphate buffer (pH 7.2) containing 2% potassium antimonate. After rising in buffer (0.1 M phosphate buffer containing 2% potassium antimonate, pH 7.2), the tissue was postfixed in 1% osmium tetroxide in 0.1 M potassium phosphate buffer containing 2% potassium antimonate for 2 h at 4°C. The tissue was dehydrated in a graded alcohol series and embedded in epoxy resin. For observation with the transmission electron microscope, ultrathin sections were prepared. Control grids mounted with tissue sections were immersed in a solution of 100 mM ethylene glycol tetraacetic acid (pH 8.0), a chelator with high affinity for Ca ions, and incubated at 60°C for 1 h. After treatment, the grids were rinsed in distilled water (Suzuki et al., 2003). Electron micrographs were taken with a Philips CM120 Biotwin Lens electron microscope at 75 kV in the Diagnostic and Research Electron Microscopy Laboratory at the University of California, Davis. All samples were exposed to the same buffers as well as processed and analyzed at the same time.

Cytosolic Ca Concentration

Cytosolic Ca concentration was analyzed in five fruit replications. Each replication was a single fruit harvested from each of five wild-type or *sCAX1*-expressing plants at 40 DAP. From each fruit, three thin, healthy subepidermal pericarp sections were manually cut from the blossom-end region with a scalpel for cytosolic Ca determination. The thin sections were incubated in the loading solution containing 100 mM KCl, 10 mM MES (pH 5.0 with KOH), 1 mM $CaCl_2$, 300 μM eserine, and 5 μM Fluo4-AM (Invitrogen) for 1 h. The negative control samples were incubated in 100 mM KCl, 10 mM MES (pH 5.0 with KOH), 300 μM eserine, 5 μM Fluo4-AM, 5 mM EGTA, and 25 μM A23187 (Supplemental Fig. S4). The fluorophores were imaged using a Zeiss LSM 5 PASCAL confocal microscope with a 488-nm argon laser (excitation), 488-nm dichroic mirror, 505- to 530-nm band-path emission filter, 10× 0.3 numerical aperture, and Neofluar objective lens (Zeiss). The pinhole setting was air unit = 1. All cell images were taken under the exact same conditions and during the same session. In each sample, cells were optically sectioned, and the images obtained were used to generate three-dimensional projection images using the brightest point projection method in the Zeiss LSM 5 PASCAL software. The edge of each cell three-dimensional projection image was manually delineated, and the average fluorescence intensity of the cell was quantified using the ImageJ program. The average fluorescence intensities were determined in a total of 15 cells in each genotype. The fluorescence intensity of each replication represents the average of the fluorescence intensity of three cells measured in each of the five fruit.

Transcriptional Analysis

The expression analysis was accomplished in three biological replications. Each biological replication included 10 fruit harvested from two wild-type or *sCAX1*-expressing plants at 15 DAP. Total RNA was extracted from blossom-end pericarp fruit tissue as described in the RNeasy Plant Mini Kit (Qiagen). The RNA concentration and purity were determined at 260 and 280 nm using a UV spectrophotometer (NanoDrop 2000; Thermo Scientific). Total RNA samples were quality assessed before beginning target preparation/processing steps by running 25 to 250 ng of each sample onto an RNA Lab-On-A-Chip (Caliper Technologies) that was evaluated on an Agilent Bioanalyzer 2100 (Agilent Technologies). Total RNA (300 ng) was processed for the microarray hybridizations using the Affymetrix GeneChip 3′ IVT Express Kit. The resultant biotinylated copy RNA was fragmented and hybridized to the GeneChip Tomato Genome Array, which contains 10,209 tomato probe sets that interrogate more than 9,200 tomato genes. The arrays were washed, stained, and scanned at the Microarray Core Facility at the University of California Davis Genome Center. The raw data were imported into R statistical software, background subtracted, and normalized with the Robust Multi-array Average method (Irizarry et al., 2003). The paired *t* test was used to calculate *P* values, which were then adjusted to cope with the problem of false discovery rates (Storey, 2002). Genes with adjusted values of $P < 0.05$ and 2-fold or greater change in expression were considered to be differentially expressed in *sCAX1*-expressing fruit pericarp tissue compared with wild-type fruit pericarp tissue (Supplemental Tables S1–S3). Annotations of differentially expressed genes were obtained by BLAST search comparisons with the National Center for Biotechnology Information (NCBI) database. Functional classifications were accomplished with the MapMan software, a user-driven tool that displays large data sets onto diagrams of metabolic pathways or other processes (Thimm et al., 2004).

RT-PCR

The RT-PCR analysis was accomplished in three biological replications. Each biological replication included 10 fruit harvested from two wild-type or *sCAX*-expressing plants. Total RNA was extracted and quantified as described before. For all samples, equal amounts of total RNA (3 μg) were reverse transcribed using SuperScript III (Invitrogen) according to the manufacturer's protocol. RT-PCR was then performed with the addition of 1× SYBR Green (Applied Biosystems) to each sample containing about 100 ng of the synthesized cDNA. The data obtained were normalized based on the expression of the housekeeping tomato 18S rRNA (Martinelli et al., 2009). All primers were designed with 20-nucleotide length and melting point temperature of 58°C ± 3°C (Supplemental Table S4). Four putative Ca^{2+}/H^+ exchangers and one Ca^{2+}/Na^+ exchanger nucleotide sequences were obtained in the tomato EST database in the NCBI GenBank (http://www.ncbi.nlm.nih.gov/GenBank/). Among these ESTs, only three Ca^{2+}/H^+ exchangers and the Ca^{2+}/Na^+ exchanger were found to be expressed in the targeted fruit tissue. The expressed nucleotide sequences were named CAX3 (NCBI: BP884739), with 83% identity to vacuolar Ca^{2+}/H^+ exchanger (NCBI: AF461691; Arabidopsis), CAX4 (NCBI: EF647616), with 86% identity to vacuolar Ca^{2+}/H^+ exchanger (NCBI: XM_002528054; *Ricinus communis*), CAX6 (NCBI: AK326847), with 75% identity to vacuolar Ca^{2+}/H^+ exchanger (NCBI: NM_001158996; *Zea mays*), and CAX7 (NCBI: AW221661), with 69% identity to Ca^{2+}/Na^+ exchanger (NCBI: NM_104200; Arabidopsis). CAX3, CAX6, and CAX7 nucleotides are part of unigene sequences. The gene sequence for one tomato *V-ATPase* (gene identifier 543862, A2 subunit) and the nucleotide sequence for a putative tomato *PPase* (NCBI: AK320752), with 84% identity to *H⁺-pyrophosphatase* (XM_002530709; *R. communis*) were also obtained in the NCBI GenBank. Eight putative Ca-ATPase unigenes obtained in the Sol Genomics Network (SGN) database (http://solgenomics.net/index.pl) were also used for expression analysis, and all eight sequences were found to be expressed in pericarp fruit tissues. The unigene sequences were named Ca-ATPase1 (SGN-U581856), with 75% identity to endoplasmic reticulum Ca-ATPase (NCBI: NM_100655; Arabidopsis), Ca-ATPase2 (SGN-U581346), with 72% identity to tonoplast Ca-ATPase (NCBI: NM_115593; Arabidopsis), Ca-ATPase3 (SGN-U571409), with 75% identity to endoplasmic reticulum Ca-ATPase (NCBI: NM_119927; Arabidopsis), Ca-ATPase4 (SGN-U568889), with 78% identity to endoplasmic reticulum Ca-ATPase (NCBI: XM_002320177; *Populus trichocarpa*), Ca-ATPase5 (SGN-U603702), with 77% identity to endoplasmic reticulum Ca-ATPase (NCBI: NM_100640; Arabidopsis), Ca-ATPase6 (SGN-U563935), with 80% identity to endoplasmic reticulum Ca-ATPase (NCBI: XM_002320646; *P. trichocarpa*), Ca-ATPase7 (SGN-U568808), with 74% identity to endoplasmic reticulum Ca-ATPase (NCBI: NM_100887; Arabidopsis), and Ca-ATPase8 (SGN-U595382), with 74% identity to endoplasmic reticulum Ca-ATPase (NCBI: NM_100887; Arabidopsis).

Statistical Analysis

The ANOVA for a completely randomized design was performed for each variable, except for the microarray data, which were analyzed as described previously. The analyses were accomplished using the SAS statistical package (SAS Institute). The mean values were compared using Duncan's test ($P = 0.05$). Values presented are means ± SE. Pearson's correlation coefficient (*r*) was calculated for the parameters apoplastic Ca × electrolyte leakage, apoplastic Ca × BER incidence, and electrolyte leakage × BER incidence.

Sequence data from this article can be found in the NCBI and SGN data libraries (NCBI: 818395, BP884739, EF647616, AK326847, AW221661, 543862, and AK320752; SGN: SGN-U581856, SGN-U581346, SGN-U571409, SGN-U568889, SGN-U603702, SGN-U563935, SGN-U568808, and SGN-U595382).

Supplemental Data

The following materials are available in the online version of this article.

Supplemental Figure S1. Ubiquitin- and autophagy-dependent degradation pathways in *sCAX1*-expressing fruit pericarp at 15 DAP.

Supplemental Figure S2. Biosynthetic pathway of cell wall precursors in *sCAX1*-expressing fruit pericarp at 15 DAP.

Supplemental Figure S3. Phenylpropanoid pathway (lignin biosynthesis) in *sCAX1*-expressing fruit pericarp at 15 DAP.

Supplemental Figure S4. Negative confocal microscopy control images.

Supplemental Table S1. Summary of genes with significant up-regulated expression in *sCAX1*-expressing fruit pericarp at 15 DAP.

Supplemental Table S2. Summary of genes with significant down-regulated expression in *sCAX1*-expressing fruit pericarp at 15 DAP.

Supplemental Table S3. Entire gene data set for GeneChip analysis.

Supplemental Table S4. Nucleotide identifier numbers and primers used for RT-PCR assays.

ACKNOWLEDGMENTS

We thank Grete N. Adamson and Patricia Kysar for valuable contributions to the electron microscopy approach used in our study.

Received February 27, 2011; accepted April 1, 2011; published April 4, 2011.

LITERATURE CITED

Abdal M, Suleiman M (2005) Blossom end rot occurrence in calcareous soil of Kuwait. Acta Hortic **695:** 63–65

Almeida DPF, Huber DJ (1999) Apoplastic pH and inorganic ion levels in tomato fruit: a potential means for regulation of cell wall metabolism during ripening. Physiol Plant **105:** 506–512

Cessna SG, Low PS (2001) An apoplastic Ca^{2+} sensor regulates internal Ca^{2+} release in aequorin-transformed tobacco cells. J Biol Chem **276:** 10655–10662

Clarkson DT, Hanson JB (1980) The mineral nutrition of higher plants. Annu Rev Plant Physiol **31:** 239–298

Edwards R, Dixon DP, Walbot V (2000) Plant glutathione S-transferases: enzymes with multiple functions in sickness and in health. Trends Plant Sci **5:** 193–198

Enoch S, Glinka Z (1983) Turgor-dependent membrane permeability in relation to calcium level. Physiol Plant **59:** 203–207

Evans HJ, Troxler RV (1953) Relation of calcium nutrition to the incidence of blossom-end rot in tomatoes. Proc Am Soc Hortic Sci **61:** 346–352

Geraldson CM (1957) Control of blossom-end rot of tomatoes. Proc Am Soc Hortic Sci **69:** 309–317

Hanson JB (1960) Impairment of respiration, ion accumulation, and ion retention in root tissue treated with ribonuclease and ethylenediamine tetraacetic acid. Plant Physiol **35:** 372–379

Hanson JB (1984) The functions of calcium in plant nutrition. *In* PB Tinker,

A Lauchli, eds, Advances in Plant Nutrition, Ed 1, Vol 1. Praeger Publishers, New York, pp 149–208

Harker FR, Venis MA (1991) Measurement of intracellular and extracellular free calcium in apple fruit cells using calcium-selective microelectrodes. Plant Cell Environ **14:** 525–530

Henley JR, Cao H, McNiven MA (1999) Participation of dynamin in the biogenesis of cytoplasmic vesicles. FASEB J (Suppl 2) **13:** S243–S247

Hepler PK (2005) Calcium: a central regulator of plant growth and development. Plant Cell **17:** 2142–2155

Hirschi KD (1999) Expression of *Arabidopsis CAX1* in tobacco: altered calcium homeostasis and increased stress sensitivity. Plant Cell **11:** 2113–2122

Hirschi KD (2004) The calcium conundrum: both versatile nutrient and specific signal. Plant Physiol **136:** 2438–2442

Hirschi KD, Zhen RG, Cunningham KW, Rea PA, Fink GR (1996) CAX1, an H^+/Ca^{2+} antiporter from Arabidopsis. Proc Natl Acad Sci USA **93:** 8782–8786

Ho LC, White PJ (2005) A cellular hypothesis for the induction of blossom-end rot in tomato fruit. Ann Bot (Lond) **95:** 571–581

Irizarry RA, Hobbs B, Collin F, Beazer-Barclay YD, Antonellis KJ, Scherf U, Speed TP (2003) Exploration, normalization, and summaries of high density oligonucleotide array probe level data. Biostatistics **4:** 249–264

Kang BH, Busse JS, Bednarek SY (2003) Members of the *Arabidopsis* dynamin-like gene family, ADL1, are essential for plant cytokinesis and polarized cell growth. Plant Cell **15:** 899–913

Kaya C, Kirnak H, Higgs D, Saltali K (2002) Supplementary calcium enhances plant growth and fruit yield in strawberry cultivars grown at high (NaCl) salinity. Sci Hortic (Amsterdam) **93:** 65–74

Lewis JD, Lazarowitz SG (2010) Arabidopsis synaptotagmin SYTA regulates endocytosis and virus movement protein cell-to-cell transport. Proc Natl Acad Sci USA **107:** 2491–2496

Love AJ, Milner JJ, Sadanandom A (2008) Timing is everything: regulatory overlap in plant cell death. Trends Plant Sci **13:** 589–595

Martinelli F, Uratsu SL, Reagan RL, Chen Y, Tricoli D, Fiehn O, Rocke DM, Gasser CS, Dandekar AM (2009) Gene regulation in parthenocarpic tomato fruit. J Exp Bot **60:** 3873–3890

Meyer GA, Keliher PN (1992) An overview of analysis by inductively coupled plasma-atomic emission spectrometry. *In* A Montaser, DW Golightly, eds, Inductively Coupled Plasmas in Analytical Atomic Spectrometry, Ed 2, Vol 1. VCH Publishers, New York, pp 473–516.

Millikan CR, Bjarnason EN, Osborn RK, Hanger BC (1971) Calcium concentration in tomato fruits in relation to the incidence of blossom-end rot. Aust J Exp Agric Anim Husb **11:** 570–575

Nonami H, Fukuyama T, Yamamoto M, Yang L, Hashimoto Y (1995) Blossom-end rot of tomato plants may not be directly caused by calcium deficiency. Acta Hortic **396:** 107–114

Olivieri F, Godoy AV, Escande A, Casalongue CA (1998) Analysis of intercellular washing fluids of potato tubers and detection of increased proteolytic activity upon fungal infection. Physiol Plant **104:** 232–238

Orvar BL, Sangwan V, Omann F, Dhindsa RS (2000) Early steps in cold sensing by plant cells: the role of actin cytoskeleton and membrane fluidity. Plant J **23:** 785–794

Park S, Cheng NH, Pittman JK, Yoo KS, Park J, Smith RH, Hirschi KD (2005a) Increased calcium levels and prolonged shelf life in tomatoes expressing Arabidopsis H^+/Ca^{2+} transporters. Plant Physiol **139:** 1194–1206

Park S, Kang TS, Kim CK, Han JS, Kim S, Smith RH, Pike LM, Hirschi KD (2005b) Genetic manipulation for enhancing calcium content in potato tuber. J Agric Food Chem **53:** 5598–5603

Park S, Kim CK, Pike LM, Smith RH, Hirschi KD (2004) Increased calcium in carrots by expression of an Arabidopsis H^+/Ca^{2+} transporter. Mol Breed **14:** 275–282

Picchioni GA, Watada AE, Conway WS, Whitaker BD, Sams CE (1998) Postharvest calcium infiltration delays membrane lipid catabolism in apple fruit. J Agric Food Chem **46:** 2452–2457

Picchioni GA, Watada AE, Whitaker BD, Reyes A (1996) Calcium delays senescence-related membrane lipid changes and increases net synthesis of membrane lipid components in shredded carrots. Postharvest Biol Technol **9:** 235–245

Plieth C (2001) Plant calcium signaling and monitoring: pros and cons and recent experimental approaches. Protoplasma **218:** 1–23

Pomper KW, Breen PJ (1995) Levels of apoplastic solutes in developing strawberry fruit. J Exp Bot **46:** 743–752

Rossignol M, Lamant A, Salsae L, Heller R (1977) Calcium fixation by the roots of calcicole and calcifuge plants: the importance of membrane systems and their lipid composition. *In* M Thellier, A Monnier, M Demarty, J Dainty, eds, Transmembrane Ionic Exchanges in Plants, Ed 1, Vol 1, Editions du CNRS, Paris/Editions de 1'Universite, Rouen, pp 483–490

Roxas VP, Smith RK Jr, Allen ER, Allen RD (1997) Overexpression of glutathione S-transferase/glutathione peroxidase enhances the growth of transgenic tobacco seedlings during stress. Nat Biotechnol **15:** 988–991

Ruan YL, Mate C, Patrick JW, Brady CJ (1995) Non-destructive collection of apoplast fluid from developing tomato fruit using a pressure dehydration procedure. Aust J Plant Physiol **22:** 761–769

Saltveit ME (2002) The rate of ion leakage from chilling-sensitive tissue does not immediately increase upon exposure to chilling temperatures. Postharvest Biol Technol **26:** 295–304

Sanders D, Pelloux J, Brownlee C, Harper JF (2002) Calcium at the crossroads of signaling. Plant Cell (Suppl) **14:** S401–S417

Saure MC (2001) Blossom-end rot of tomato (*Lycopersicon esculentum* Mill.): a calcium or a stress-related disorder? Sci Hortic (Amsterdam) **90:** 193–208

Schapire AL, Voigt B, Jasik J, Rosado A, Lopez-Cobollo R, Menzel D, Salinas J, Mancuso S, Valpuesta V, Baluska F, et al (2008) *Arabidopsis* synaptotagmin 1 is required for the maintenance of plasma membrane integrity and cell viability. Plant Cell **20:** 3374–3388

Shulaev V, Cortes D, Miller G, Mittler R (2008) Metabolomics for plant stress response. Physiol Plant **132:** 199–208

Simon EW (1978) The symptoms of calcium deficiency in plants. New Phytol **80:** 1–15

Storey JD (2002) A direct approach to false discovery rates. J R Stat Soc B **64:** 479–498

Suzuki K, Shono M, Egawa Y (2003) Localization of calcium in the pericarp cells of tomato fruits during the development of blossom-end rot. Protoplasma **222:** 149–156

Thimm O, Bläsing O, Gibon Y, Nagel A, Meyer S, Krüger P, Selbig J, Müller LA, Rhee SY, Stitt M (2004) MAPMAN: a user-driven tool to display genomics data sets onto diagrams of metabolic pathways and other biological processes. Plant J **37:** 914–939

Tuna AL, Kaya C, Ashraf M, Altunlu H, Yokas I, Yagmur B (2007) The effects of calcium sulphate on growth, membrane stability and nutrient uptake of tomato plants grown under salt stress. Environ Exp Bot **59:** 173–178

Tuteja N, Mahajan S (2007) Calcium signaling network in plants: an overview. Plant Signal Behav **2:** 79–85

Wada H, Shackel KA, Matthews MA (2008) Fruit ripening in *Vitis vinifera*: apoplastic solute accumulation accounts for pre-veraison turgor loss in berries. Planta **227:** 1351–1361

Wang W, Vinocur B, Shoseyov O, Altman A (2004) Role of plant heat-shock proteins and molecular chaperones in the abiotic stress response. Trends Plant Sci **9:** 244–252

Welbaum GE, Meinzer FC (1990) Compartmentation of solutes and water in developing sugarcane stalk tissue. Plant Physiol **93:** 1147–1153

White PJ (2000) Calcium channels in higher plants. Biochim Biophys Acta **1465:** 171–189

White PJ, Broadley MR (2003) Calcium in plants. Ann Bot (Lond) **92:** 487–511

Yoshida K, Kaothien P, Matsui T, Kawaoka A, Shinmyo A (2003) Molecular biology and application of plant peroxidase genes. Appl Microbiol Biotechnol **60:** 665–670

Zhang R, Kang KA, Piao MJ, Chang WY, Maeng YH, Chae S, Lee IK, Kim BJ, Hyun JW (2010) Butin reduces oxidative stress-induced mitochondrial dysfunction via scavenging of reactive oxygen species. Food Chem Toxicol **48:** 922–927

Zhou L, Fu Y, Yang Z (2009) A genome-wide functional characterization of *Arabidopsis* regulatory calcium sensors in pollen tubes. J Integr Plant Biol **51:** 751–761